Cluster-Based Non-Stationary Vehicular Channel Model

Zhinan Xu, Mingming Gan, Thomas Zemen
AIT Austrian Institute of Technology, Vienna, Austria

***Abstract*—Vehicular communication channels are characterized by a time- and frequency-selective non-stationary fading process. The real-time simulation of this fading process is addressed in this paper. We analyze the clustering of multi-path components in the delay-Doppler domain using the local scattering function of channel measurement data. For the statistical analysis, we divide the cluster locations in the delay-Doppler plane into different characteristic regions. The time-variant cluster parameters, such as cluster birth rate, relationship between delay and Doppler shift, and the distribution of the lifetime and of the cluster gain in each region, are characterized. For low complexity emulation the cluster parameters are randomly drawn from this pre-computed distributions. Our model is validated with measurement data using the cumulative distribution function of the root mean square delay spread and Doppler spread. A close match of our numeric model with measurement results is demonstrated.**

I. Introduction

For the design of reliable vehicular communication systems, a comprehensive understanding of the true propagation conditions of vehicular radio channels is required. As shown by vehicular radio channel measurements at 5 GHz, the impulse response of vehicular channels is composed of (1) a multi-path component (MPC) stemming from the line-of-sight (LOS), (2) specular scattering, and (3) diffuse scattering at objects in the environment. The delay and Doppler of each MPC changes with time due to the fast movement of both the transmitter (TX) and receiver (RX). Hence, the statistical properties of the vehicular channel change over time and therefore the channel is non-stationary [1], [2]. For this reason, the commonly used tap delay line channel model [3] with fixed power delay-profile (PDP) and Doppler spectral-density (DSD) is *not* suitable for vehicular communications.

In order to obtain realistic link level simulation results, we need a non-stationary channel model that resembles the true propagation conditions. Because of that, a vehicular non-stationary geometry-based stochastic channel model (GSCM), has been developed for highway [4] and intersection [5] scenarios, where point scatterers are randomly placed according to a certain spatial distribution. However, the complexity of a GSCM is high due to the summation of a large number of complex exponentials (see [5, (14)]). In [6] a low complexity two path channel is used for testing transceivers with a real-time wireless software defined radio (SDR) channel emulator. We will extend the concept of [6] with more realistic settings in this paper.

This work was partly performed in the FTW project Future ITS, a scientific cooperation co-funded by Kapsch TrafficCom AG, and Vienna University of Technology.

Contribution of the Paper:

- We develop a cluster-based [7], [8] vehicular channel model with low computational complexity suitable for a real-time implementation. The relevant time-variant parameters, e.g., cluster birth rate, relationship between delay and Doppler shift, and the distributions of lifetime and of cluster gain, are characterized based on measurements.
- We perform the clustering algorithm using a delay-Doppler power spectral density estimate in form of the local scattering function (LSF) [1]. MPCs having similar delay and Doppler shift will form a cluster. The time-variant cluster parameters are obtained from a cluster identification-and-tracking algorithm. These parameters serve as input parameters of our channel model.
- We divide the cluster locations into different regions based on the relationship between delay and Doppler shift.
- We validate the proposed model by comparing the cumulative distribution function (CDF) of the root mean square (RMS) delay spread and of RMS Doppler spread showing a good match.

II. Cluster Identification and Tracking

A. Local Scattering Function

The vehicular propagation conditions measured by the time-variant frequency response $g(t, f)$ change rapidly due to the high velocities of the TX and RX. Thus, the observed sampled fading process $g[m, q] = g(mt_s, qB/N)$ is non-stationary, where t_s is the sampling interval in time, B is the channel bandwidth, N denotes the number of samples in the frequency domain, m is the discrete time index and n is the delay index, respectively.

Due to the finite rate of the environment changes, the non-stationarity can be overcome by approximating the fading process to be locally wide-sense stationary for a region with finite extent in time and frequency [9]. The local stationarity region is defined as having $M \times N$ samples in time and frequency, respectively. For each stationarity region we are now able to calculate the LSF [1], [10], see Fig. 1.

The total number of snapshots and frequency bins within one measurement run are denoted by S and Q, respectively. Therefore, the time index of each stationarity region

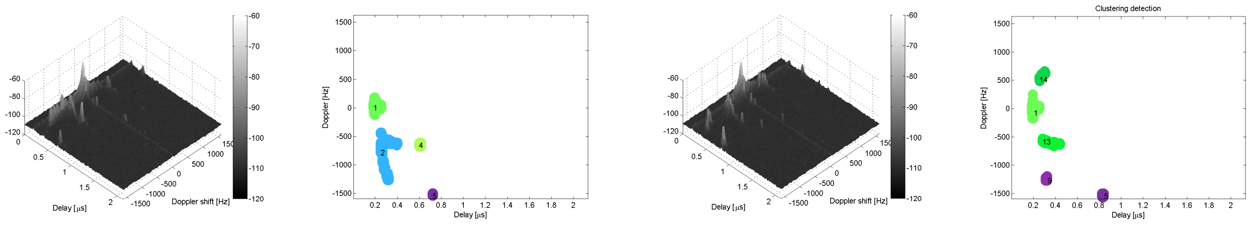

(a) Local scattering function at $k_{t,0}$ (b) Cluster identification $k_{t,0}$ (c) Local scattering function at $k_{t,1}$ (d) Cluster identification $k_{t,1}$

Fig. 1. Local scattering function and identified clusters at two different time instants $k_{t,0}$ and $k_{t,1}$

is $k_t \in \{0, \cdots, \lfloor S/M - 1 \rfloor\}$, and the frequency index of each stationarity region is $k_f \in \{0, \cdots, \lfloor Q/N - 1 \rfloor\}$. k_t and k_f correspond to the center of each stationarity region. An estimate of the discrete LSF is defined as $\hat{C}[k_t, k_f; n, p]$ [1], where $n \in \{0, \cdots, N-1\}$ is the delay index, and $p \in \{-M/2, \cdots, M/2-1\}$ is the Doppler index. In our work, we are interested in $\hat{C}[k_t; n, p]$, where $k_f = 0$ because of $Q = N$. The LSF $\hat{C}[k_t; n, p]$ is a time-varying representation of the delay-Doppler spectral density. In order to consistently characterize the evolution of cluster parameters over time, we now introduce our cluster identification and tracking algorithm.

B. Data Preprocessing

We are only interested in relevant MPCs above a certain power level. In the first step, we identify these MPCs in the LSF, employing the power threshold criterion [11], where two power thresholds are used. A MPC exists if both of the following two criteria are satisfied: (1) the power of the MPC is γ dB above the noise floor, and (2) the power of the MPC is not more than κ dB below the highest detected peak. In this work, we choose $\gamma = 10$ and $\kappa = 25$. The MPCs which do not satisfy the above criteria are set to zero.

C. Cluster Identification

In order to identify the clusters formed by the relevant MPCs, the DBSCAN algorithm [12] is used, which is a density based clustering algorithm to discover clusters of arbitrary shape. DBSCAN requires only two input parameters, i.e. the neighborhood radius ϵ and the minimum number of objects in a neighborhood $p_{\min}$.

D. Cluster Tracking

The purpose of tracking is to capture the evolution of the cluster centroid movement and the time-variant cluster spreads in delay $S_{\tau,\ell}[k_t]$ and Doppler $S_{\nu,\ell}[k_t]$. The algorithm is based on the multi-path component distance (MCD) [13] measure of the cluster centroids. At time instant k_t, $L[k_t]$ cluster centroids $\mu_\ell[k_t] = [\theta_\ell[k_t], \mu_\ell[k_t]]^{\mathrm{T}}$ are detected, where $\ell \in \{1, \ldots, L(k_t)\}$. The current stationarity region is denoted by k_t and the previous one by $k_t - 1$. The algorithm proceeds as follows:

1) The MCD between any old (at time $k_t - 1$) and any new centroids (at time k_t) is calculated.
2) If the distance between a new centroid and its closest old centroid is larger than a predefined threshold, the new centroid is regarded as a newly detected centroid.
3) For each old centroid, the number of new centroids within the threshold c is checked:
   - If $c = 1$, the old centroid is moved.
   - If $c > 1$, the old centroid splits. The closest new one is regarded as old moved centroid. All others are treated as new centroids.

Figure 1 shows the local scattering function and the identified clusters of an exemplary vehicular channel measurement in the delay-Doppler domain at two different time instants. Each cluster is colored according to the cluster ID given by the tracking algorithm. At time instant $k_{t,0}$, four clusters are detected. Cluster 1 corresponds to the LOS component, which exists in both time instants. Cluster 5 stemming from the vehicle in the opposite direction, appears also in both time instants. However the position of Cluster 5 is changed due to the movements of the vehicles. Cluster 2 disappears and splits into several clusters at $k_{t,1}$.

III. Measurement Scenarios and Data

The measurements used in the present work were collected in the DRIVEWAY'09 measurement campaign [14] conducted in Lund, Sweden. The channel impulse response is measured with a time resolution of $t_{\mathrm{s}} = 307.2\,\mu$s. The total time interval is $T = 10$ s. Therefore, there are $S = 32000$ snapshots in total. The carrier frequency is $f_{\mathrm{c}} = 5.6$ GHz within a bandwidth of $B = 240$ MHz. Both TX and RX car are equipped with a linear array with four circular polarized patch antennas perpendicular to the driving direction. The antennas cover the four main propagation directions due to their main lobes [15]. In order to achieve a $360°$ coverage in the azimuth plane, we consider to combine the antenna radiation pattern in this paper.

In this paper we present results for a scenario where a truck is obstructing the line-of-sight (LOS) between the TX and RX drive that drive in the same direction on a highway at around 75 km/h. The TX drives in front. In addition, there is a truck in the front of the Tx. A 2-D top view of this scenario is shown in Fig. 2. There are some traffic signs along the highway. Meanwhile, some vehicles drive in the opposite direction on the other lane of the highway.

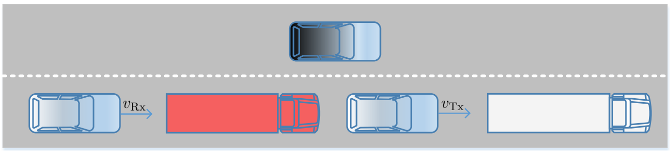

Fig. 2. LOS Obstruction Scenario

TABLE I
CONDITIONAL PROBABILITY

	Newly Born Clusters			
N	0	1	2	3
1	0.750	0.212	0.019	0.019
2	0.667	0.289	0.044	0
3	0.696	0.130	0.174	0
4	0.500	0.389	0.111	0
5	0.425	0.375	0.125	0.075
6	0.421	0.474	0.105	0
7	0.500	0.500	0	0
8	1	0	0	0

IV. Non-Stationary Cluster Model

We represent the sampled time-variant frequency response as superposition of clusters for the stationarity region k_t

$$g[m,q] = g[k_tM+m',q] = g_{\text{Tx}}[q]g_{\text{Rx}}[q] \cdot \sum_{\ell=0}^{L[k_t]} \alpha_\ell[k_t]\mathrm{e}^{-\mathrm{j}2\pi\theta_\ell[k_t]q}\mathrm{e}^{\mathrm{j}2\pi\nu_\ell[k_t]m'}, \quad (1)$$

where ℓ is the cluster index, N denotes the number of clusters, $\theta_\ell = \tau_\ell B/N$ is the normalized delay of the centroid of the ℓ-th cluster, α_ℓ is the average amplitude, and $\nu_\ell = f_\ell M t_s$ is the normalized Doppler shift.

For comparison purposes, we employ a bandwidth $B = 240\,\text{MHz}$ and $N = 769$ frequency bins in accordance to the bandwidth and number of frequency samples of the measurement, $T_{\text{C}} = 1/B$.

A. Cluster Parameters

For the cluster model (1) we need to obtain the cluster parameters N, α, θ, and ν for each stationarity region k_t from the associated LSF.

1) Birth Rate Evaluation: Firstly, the birth rate of the newly born clusters is calculated. In order to model the trend of the number of clusters more accurately, we evaluate the birth rate of the the newly born clusters at k_t based on the number of clusters $L[k_t-1]$. With $L[k_t-1]$, we can obtain the conditional probabilities of having different number of new clusters at stationary region k_t. In Tab. I, the conditional probabilities are shown. The obtained conditional probabilities will be used to generate the number of clusters at each stationary time region in the proposed model.

2) Relationship Between Delay and Doppler Shift: Considering two vehicles moving on a highway with constant speeds, two vehicles can be placed on the x-axis as shown in [16, Fig. 1], where the origin of the coordinate system is placed halfway between vehicles.

Due to the movement of the both vehicles, their positions are changing with time. The position $\boldsymbol{x}(t) = [x(t), y(t)]^{\text{T}}$ of both vehicles can be expressed as

$$\boldsymbol{x}_{\text{TX}}(t) = \boldsymbol{x}_{\text{t0}} + \boldsymbol{v}_{\text{TX}}t \quad (2)$$

$$\boldsymbol{x}_{\text{RX}}(t) = \boldsymbol{x}_{\text{r0}} + \boldsymbol{v}_{\text{RX}}t \quad (3)$$

where $\boldsymbol{x}_{\text{t0}} = [-d/2, 0]^{\text{T}}$ and $\boldsymbol{x}_{\text{r0}} = [d/2, 0]^{\text{T}}$ are the initial positions of the TX and RX vehicles, $\boldsymbol{v}_{\text{TX}}$ and $\boldsymbol{v}_{\text{RX}}$ are the corresponding velocity vectors. The distance $d_{\text{SC}}(\boldsymbol{x}, t)$ is the distance where the transmitted signal travels between the moving TX and RX over a scatterer located at $\boldsymbol{x}$. Depending on the geometrical description, $d_{\text{SC}}(\boldsymbol{x}, t)$ can be expressed as

$$d_{\text{SC}}(\boldsymbol{x}, t) = d_{\text{t}}(\boldsymbol{x}, t) + d_{\text{r}}(\boldsymbol{x}, t) \quad (4)$$

where $d_{\text{t}}(\boldsymbol{x}, t)$ is the distance between TX and the scatterer and $d_{\text{r}}(\boldsymbol{x}, t)$ is the distance between RX and the scatterer, respectively. Therefore, the transmitted signal experiences a delay

$$\tau_{\text{SC}}(\boldsymbol{x}, t) = d_{\text{SC}}(\boldsymbol{x}, t)/c_0\,, \quad (5)$$

where c_0 is the speed of light. In [16, Fig. 1], an ellipse with two vehicles in its foci represents locations of scatterers causing the same delay. In addition, the transmitted signal also experiences a Doppler shift due to the movement of vehicles, which can be obtained by

$$\nu_{\text{SC}}(\beta(t), t) = \left(||\boldsymbol{v}_{\text{TX}}|| \cos(\beta(t)) + ||\boldsymbol{v}_{\text{RX}}|| \cos(\varphi(t))\right) f_{\text{C}}/c_0 \quad (6)$$

where β is the angle between the velocity vector $\boldsymbol{v}_{\text{TX}}$ and the line connecting the TX and the scatterer, φ is the angle between the velocity vector $\boldsymbol{v}_{\text{RX}}$ and the line connecting the RX and the scatterer, and f_{C} is the center frequency. Thus, the delay and Doppler shift has a certain relationship, which depends on the positions and velocities of the TX and RX, and the location of the scatterer. In Fig. 3, we give an example of the relationship between the delay and Doppler shift. The contributions of different scatterers lie on different 'U' shapes on the delay Doppler plane. We can use this concept to obtain the delay and Doppler shift values of the cluster in our proposed model. The premise is that the velocities of TX and RX, and the location of the cluster are known.

3) Region Division: Based on the relationship between delay and Doppler shift, we can divide the cluster locations into four regions as shown in Fig. 4. In Table II, we obtain the probabilities of clusters located in different regions according to the number of detected clusters in each region. These probabilities can help to decide the cluster locations in the proposed channel model.

We place a LOS cluster in the proposed model due to the fact that the cluster related to the LOS component in 'Region 1' exists throughout the whole measurement run. Therefore, in Tab. II, we do not calculate the probability of the cluster located in 'Region 1'.

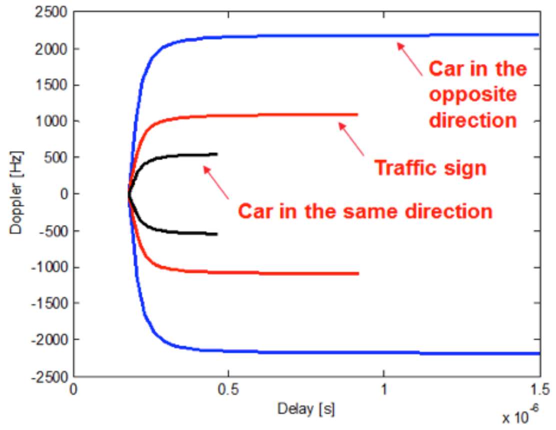

Fig. 3. Exemplary relationship between delay and Doppler shift.

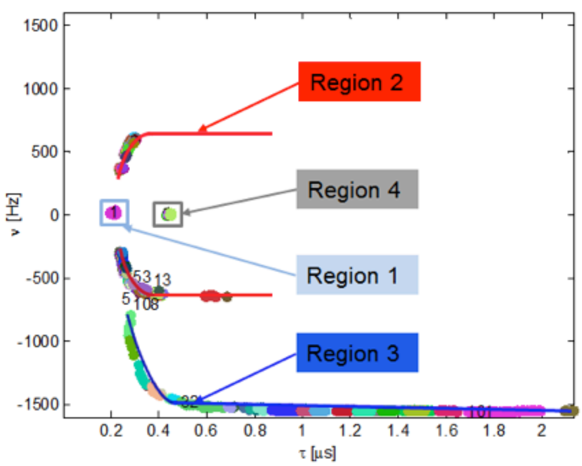

Fig. 4. Cluster locations division.

4) Distributions of Lifetime and Gain in Different Regions: After dividing the cluster locations into four regions, we analyze the distributions of cluster lifetime and gain in each region. Since the LOS cluster appears throughout the whole measurement, we only need to evaluate the distribution of the cluster gain for 'Region 1'. We found that the distribution of cluster lifetime obeys a lognormal distribution, and the distribution of cluster gain obeys a generalized extreme value distribution for the other three regions. The detailed parameters are given in Tab. III.

B. Implementation of the Non-Stationary Cluster Model

To be able to incorporate our model in a practical environment, we make the following assumptions. We consider two vehicles on a highway moving parallel to each other with constant velocities v_{TX} and v_{RX}. The vehicles on the opposite direction travel at the same speed of v_0. To simplify the problem, we assume a distance of $d_{\text{lanes}} = 10\,\text{m}$ between the two lanes according to the environment. We assume the traffic signs are also $d_{\text{signs}} = 10\,\text{m}$ away next to the lane of TX and Rx.

TABLE II
CLUSTER PROBABILITY FOR THE DIFFERENT REGIONS

Region	1	2	3	4
Probability	-	0.69	0.24	0.07

TABLE III
DISTRIBUTION PARAMETERS FOR CLUSTER LIFETIME AND GAIN

Region	lifetime (log normal) μ	σ	gain (gen. extreme value) k	σ	μ
1	-	-	-0.35	2.60e-5	10.2e-5
2	0.81	0.85	0.56	2.24e-6	2.88e-5
3	1.55	0.82	0.25	6.23e-6	3.40e-5
4	1.14	1.07	0.1	8.06e-7	2.75e-5

1) LOS Cluster: We observed that the LOS exists throughout the whole measurement run. Therefore, we assume a permanently existing LOS cluster in the delay-Doppler plane. The delay is given by the distance between the TX and RX vehicles. The power of the LOS cluster for each k_t is randomly drawn from the fitted power distribution.

2) Other Clusters: For each stationary time region k_t, we draw a random number of newly born clusters N according to the conditional probabilities obtained in Table I. For each newly born cluster, it will be associated with four key parameters, i.e., delay θ, Doppler ν, lifetime and amplitude α following the next steps:

1) We allocate each new cluster to a region according to probabilities in Table II.
2) The lifetime of the cluster is drawn from the corresponding fitted distributions obtained in Table III.
3) The power of the cluster is drawn from the corresponding power distribution in Table III.
4) We place the new cluster in a random position in the region. The relationship between delay and Doppler follows from (5) and (6).
5) If the lifetime of a new cluster is longer than one stationarity region, the geometrical position and the movement of the cluster in the delay-Doppler plane is updated using (2)-(6).

The same process is repeated for all $L[k_t]$ new clusters for every stationary region k_t. The parameters obtained for each cluster are inserted in (1) to generate the channel impulse response.

V. SIMULATION RESULTS

In order to resemble the true environment, we assign the following velocities $v_{\text{TX}} = 65\,\text{km/h}$, $v_{\text{RX}} = 65\,\text{km/h}$, $v_0 = 70\,\text{km/h}$, and the initial distance between the TX and the RX $d_{\text{intv}} = 60\,\text{m}$. To evaluate the accuracy of our proposed channel model, we compare the CDFs of the RMS delay and Doppler spread based on the proposed model and the measurements data in Fig. 5. The CDFs match quite well with the measurements.

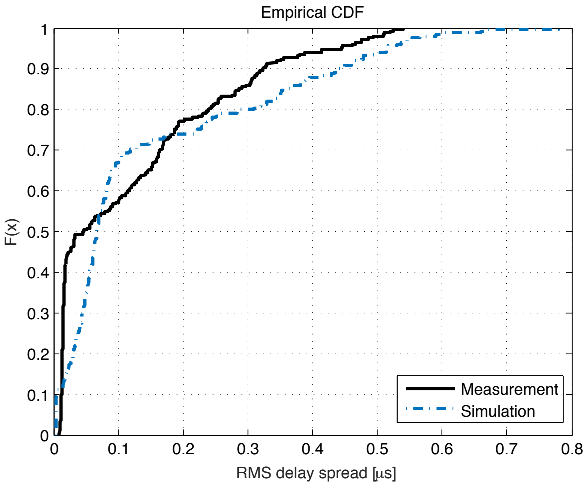

Fig. 5. RMS delay spread CDF.

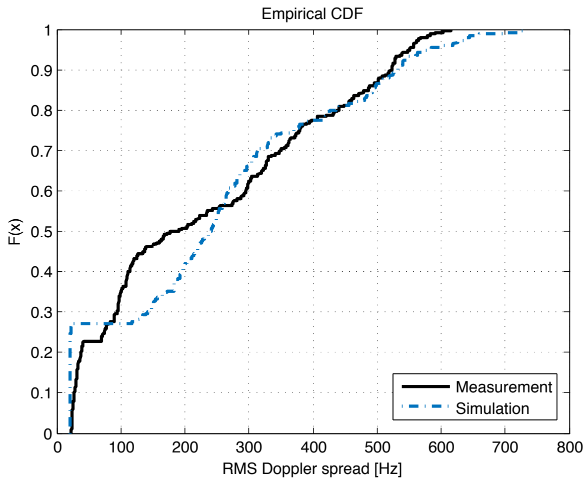

Fig. 6. RMS Doppler spread CDF.

VI. Conclusion

For non-stationary vehicular channel emulation we proposed a joint cluster identification-and-tracking approach based on the LSF. The DBSCAN algorithm was used for the cluster identification, and a low-complexity tracking algorithm relying on the MCD measure was applied to track the cluster centroids. We divided the cluster locations into different regions based on the relationship between delay and Doppler shift. The relevant time-variant parameters, e.g., cluster birth rate, relationship between delay and Doppler shift, and the distributions of lifetime and of cluster gain, were characterized. Based on these time-variant parameters, we developed a cluster-based vehicular channel model. It was validated with measurements by comparing the CDF of the RMS delay spread and RMS Doppler spread demonstrating a good match.

References

[1] L. Bernadó, T. Zemen, F. Tufvesson, A. Molisch, and C. Mecklenbräuker, "Delay and Doppler spreads of nonstationary vehicular channels for safety-relevant scenarios," *IEEE Trans. Veh. Technol.*, vol. 63, no. 1, pp. 82–93, Jan. 2014.

[2] O. Renaudin, V.-M. Kolmonen, P. Vainikainen, and C. Oestges, "Non-stationary narrowband MIMO inter-vehicle channel characterization in the 5-GHz band," *IEEE Trans. Veh. Technol.*, vol. 59, no. 4, pp. 2007–2015, May 2010.

[3] G. Acosta-Marum and M. A. Ingram, "Six time- and frequency-selective empirical channel models for vehicular wireless LANs," *IEEE Veh. Technol. Mag.*, vol. 2, no. 4, pp. 4–11, 2007.

[4] J. Karedal, F. Tufvesson, N. Czink, A. Paier, C. Dumard, T. Zemen, C. F. Mecklenbräuker, and A. F. Molisch, "A geometry-based stochastic MIMO model for vehicle-to-vehicle communications," *IEEE Trans. Wireless Commun.*, vol. 8, no. 7, pp. 3646–3657, July 2009.

[5] Z. Xu, L. Bernadó, M. Gan, M. Hofer, T. Abbas, V. Shivaldova, K. Mahler, D. Smely, and T. Zemen, "Relaying for ieee 802.11p at road intersection using a vehicular non-stationary channel model," in *6th International Symposium on Wireless Vehicular Communications (WIVEC 2014)*, Vancouver, Canada, September 2014.

[6] D. Vlastaras, S. Malkowsky, and F. Tufvesson, "Stress test of vehicular communication transceivers using software defined radio," COST IC1004, 12th Management Committee Meeting, Dublin, Ireland, January 2015.

[7] M. Gan, Z. Xu, C. F. Mecklenbräuker, and T. Zemen, "Cluster lifetime characterization for vehicular communication channels," in *9th European Conference on Antennas and Propagation (EuCAP)*, Lisbon, Portugal, April 2015.

[8] Z. Xu, M. Gan, C. F. Mecklenbräuker, and T. Zemen, "Cluster spreads for time-variant vehicular channels," in *9th European Conference on Antennas and Propagation (EuCAP)*, Lisbon, Portugal, April 2015.

[9] L. Bernadó, T. Zemen, F. Tufvesson, A. F. Molisch, and C. F. Mecklenbräuker, "The (in-)validity of the WSSUS assumption in vehicular radio channels," in *IEEE 23rd International Symposium on Personal, Indoor and Mobile Radio Communications (PIMRC)*, Sydney, Australia, September 2012.

[10] G. Matz, "On non-WSSUS wireless fading channels," *IEEE Trans. Wireless Commun.*, vol. 4, no. 5, pp. 2465–2478, September 2005.

[11] L. Bernadó, A. Roma, N. Czink, J. Karedal, A. Paier, and T. Zemen, "Cluster-Based Scatterer Identification and Characterization in Vehicular Channels," in *European Wireless Conference*, Vienna, Austria, April 2011.

[12] M. Ester, H. Kriegel, J. Sander, and X. Xu, "A density-based algorithm for discovering clusters in large spatial databases with noise," *Kdd*, 1996.

[13] N. Czink, T. Zemen, J.-P. Nuutinen, J. Ylitalo, and E. Bonek, "A time-variant MIMO channel model directly parametrised from measurements," *EURASIP Journal on Wireless Communications and Networking*, vol. 2009, 2009.

[14] A. Paier, L. Bernadó, J. Karedal, O. Klemp, and A. Kwoczek, "Overview of vehicle-to-vehicle radio channel measurements for collision avoidance applications," in *IEEE 71st Vehicular Technology Conference (VTC)*, Taipei, Taiwan, May 2010.

[15] A. Thiel, O. Klemp, A. Paiera, L. Bernado, J. Karedal, and A. Kwoczek, "In-situ vehicular antenna integration and design aspects for vehicle-to-vehicle communications," in *4th European Conference on Antennas and Propagation (EuCAP)*, April 2010.

[16] M. Walter, D. Shutin, and U.-C. Fiebig, "Delay-dependent doppler probability density functions for vehicle-to-vehicle scatter channels," *IEEE Trans. Antennas Propag.*, vol. 62, no. 4, pp. 2238–2249, April 2014.